*Characterization and Application of Nanomaterials*2024, 7(2), 6046.
https://doi.org/10.24294/can.v7i2.6046

Article

Mechanical properties of spinel ($MgCr_2O_4$) phase containing alumino-silicate glass-ceramic

Mrinmoy Garai[1,*], Arianit A. Reka[2], Shibayan Roy[1]

[1] Materials Science Center, Indian Institute of Technology (IIT), Kharagpur 600036, India
[2] Department of Chemistry, Faculty of Natural Sciences and Mathematics, University of Tetova, Tetovo 1200, North Macedonia
*** Corresponding author:** Mrinmoy Garai, mrinmoygarai@iitkgp.ac.in

CITATION

Garai M, Reka AA, Roy S. Mechanical properties of spinel ($MgCr_2O_4$) phase containing alumino-silicate glass-ceramic. Characterization and Application of Nanomaterials. 2024; 7(2): 6046. https://doi.org/10.24294/can.v7i2.6046

ARTICLE INFO

Received: 26 April 2024
Accepted: 9 July 2024
Available online: 1 August 2024

Abstract: This research study explores the addition of chromium (Cr^{6+}) ions as a nucleating agent in the alumino-silicate-glass (ASG) system (i.e., Al_2O_3-SiO_2-MgO-B_2O_3-K_2O-F). The important feature of this study is the induction of nucleation/crystallization in the base glass matrix on addition of Cr^{6+} content under annealing heat treatment (600 ± 10 °C) only. The melt-quenched glass is found to be amorphous, which in the presence of Cr^{6+} ions became crystalline with a predominant crystalline phase, Spinel ($MgCr_2O_4$). Microstructural experiment revealed the development of 200–500 nm crystallite particles in Cr^{6+}-doped glass-ceramic matrix, and such type microstructure governed the mechanical properties. The machinability of the Cr-doped glass-ceramic was thereby higher compared to base alumino-silicate glass (ASG). From the nano-indentation experiment, the Young's modulus was estimated 25(±10) GPa for base glass and increased to 894(±21) GPa for Cr-doped glass ceramics. Similarly, the microhardness for the base glass was 0.6(±0.5) GPa (nano-indentation measurements) and 3.63(±0.18) GPa (micro-indentation measurements). And that found increased to 8.4(±2.3) (nano-indentation measurements) and 3.94(±0.20) GPa (micro-indentation measurements) for Cr-containing glass ceramic.

Keywords: alumino-silicate glass; nucleation; microstructure; microhardness

1. Introduction

Al_2O_3-SiO_2-MgO-B_2O_3-K_2O-F (alumino-silicate-glass) is converted into corresponding glass-ceramic/glass-ceramic composite with typical microstructure-driven mechanical properties [1–3]. In practice, a heat-treatment schedule is followed for converting such silicate-based glass into corresponding glass-ceramic [4,5]. However, the heat treatment requires specified time and electrical energy. It is thus desired to get the glass crystallized with the least energy, i.e., without performing any heat treatment [4,6]. For this purpose, self-nucleation during the glass melting or annealing is desired. K_2O-MgO-B_2O_3-SiO_2-F systems have the ability to incorporate active ions (like chromium, aluminum, lanthanoids, etc.) at various concentrations, making it easier to provide bulk samples compared to crystalline materials. In order to add chromium ions in silicate (SiO_2)-based glasses, it can possess variable oxidation states, viz. +2, +3, +6, etc. Cr^{3+} serves as a modifier, whereas Cr^{6+} (i.e., CrO_4^{2-} structural units) can act as the glass network former [3,4]. Since chromium ions have multi-oxidation states Cr^{n+}(n = 2–6), the mechanical properties depend on its structural units (i.e., properties of the former and modifier). As the glasses possess no long-range order, the position of Cr-ions can vary depending on the ligand's locations as well as the coordination number and the average distance of the central ion-ligand [6–8]. It is reported that the higher valent chromium ion (i.e., Cr^{6+}) is effective for the

crystallization as well as microstructure in boro-silicate/alumino-silicate glass [7–9]. If nucleation in Al_2O_3-SiO_2-MgO-B_2O_3-K_2O-F glass occurs during melting or annealing temperature, glass-ceramic composite-type material is obtained instead of getting superior glass phase [6–8]. In the study on SiO_2-B_2O_3-based glass systems, Aktas et al. [8] demonstrated that 0–1 wt% Cr_2O_3-containing glass is completely amorphous, but Cr_2O_3 contents >1 wt% make those glasses crystalline, i.e., glass-ceramic. However, the effectiveness of such a technique comes from creating a finely structured crystalline phase with random orientation, typically free from pits, dents, voids, micro-cracks, or porosity [7,10]. And such a fine grain type of microstructure can generate the desired mechanical properties in final glass ceramics.

In this report, the substitution of Al^{3+} ions by Cr^{6+} ions in alumino-silicate glass (ASG), i.e., Al_2O_3-SiO_2-MgO-B_2O_3-K_2O-F system, is studied. Due to the Cr^{6+} addition in such glass, the relevant variation of the crystallization features (XRD, FESEM) is interrelated with mechanical properties (microhardness, Youngs modulus, contact depth) [4].

2. Experimental

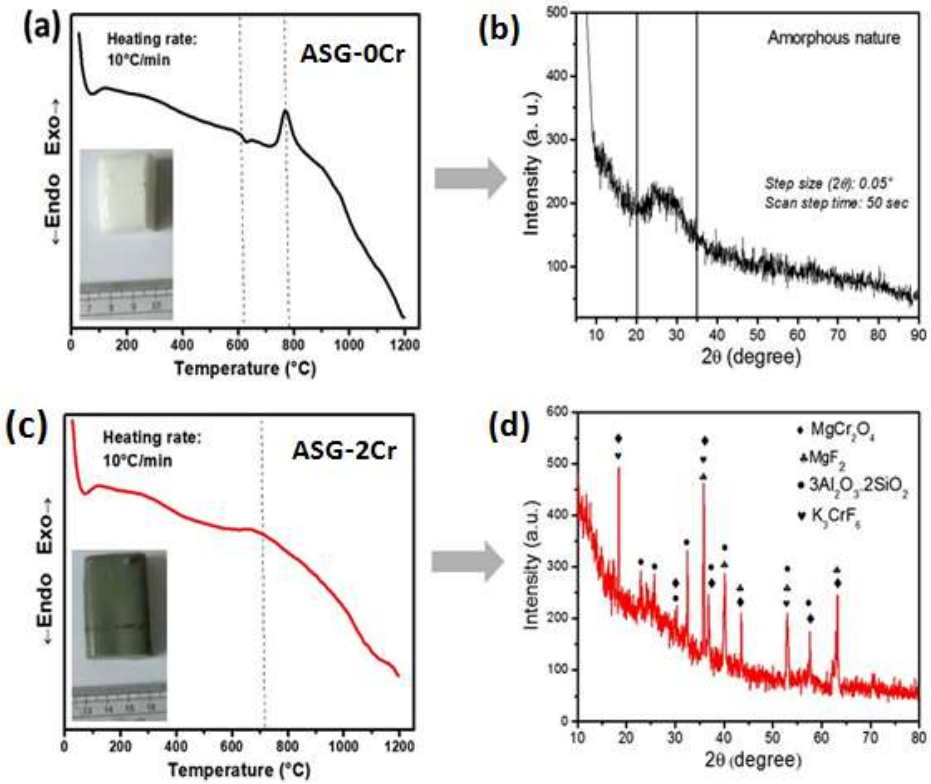

Figure 1. Differential scanning calorimetric (DSC) thermogram of Al_2O_3-SiO_2-MgO-B_2O_3-K_2O-F glass containing. **(a)** 0 mol%; **(c)** 2 mol% chromium content (inset of **Figure 1a,c** shows the photograph of corresponding glasses) and XRD pattern **(b)** 0 mol%; **(d)** 2 mol% Cr-doped glasses [4].

Two alumino-silicate-glass (ASG) of composition (mol%) (i) ASG-0Cr (7K_2O-20MgO-10B_2O_3-44SiO_2-12MgF_2-7Al_2O_3) and (ii) ASG-2Cr (7K_2O-20MgO-10B_2O_3-44SiO_2-12MgF_2-5Al_2O_3-2$K_2Cr_2O_7$) were synthesized by melt-casting using pure

chemicals, i.e., SiO_2, $Al(OH)_3$, $Mg(OH)_2$, H_3BO_3,K_2CO_3, MgF_2, and $K_2Cr_2O_7$. The details/purity of reagents are described in a previous report on a similar glass system [4]. The glasses were melted in a platinum (Pt) crucible in an electrically heated furnace at 1570(±10) °C for 2 h, followed by casting in graphite mold and thereafter annealing at 600(±10) °C (2 h). The photographs of the annealed glasses are exhibited in the inset of **Figure 1** that clearly demonstrates the opaque nature [4]. Annealed glass was characterized for microstructural and mechanical properties using the techniques of differential scanning calorimetry (DSC), X-ray diffraction (XRD), field emission scanning electron microscopy (FESEM), energy dispersive X-ray spectroscopy (EDX), nanoindentation, and Vickers microindentation [11–15].

Finely powdered (particle size < 60 μm) ASG samples were subjected to differential scanning calorimetry (DSC SetaramLabsys, Setaram Instrumentation, France) at a heating rate of 10 °C/min to obtain the phase transformation temperature. XRD analysis was recorded using an XPERTPRO MPD diffractometer (PANalytical, Netherlands) operating with Ni-filtered CuKα = 1.5406 Å radiation as the X-ray source. The morphology of the glasses (chemically etched by 2 vol.% aqueous HF solution for 10 min) was examined using a FESEM (model S430i, LEO, CEA, USA). To dictate the elements present in the synthesized glass, qualitative elemental composition analysis was performed using the energy dispersive X-ray spectroscopy (EDX) detector attached to the FESEM microscope [11,12]. Nano-indentation was taken using polished glass samples by the Berkovich indenter tip (radius = 100 nm & angle = 142.3°) Hystron, Model No. TIN 50 Triboindenter, USA. The indentation was carried out with an applied force of 5 mN under a dwell time of 10 s followed by constant unloading. The indentations were obtained from various locations within the specimen surface. For measurement, a total of 20 indentations were taken at any given location following a 4 × 5 square matrix pattern. Standard indentation P-h curves were generated from the load (*P*) controlled nano-indentation tests and the corresponding measurements of indentation depth (*h*). The microhardness (*H*) and Young's modulus (*E*) were determined from the P-h curves based on the Oliver-Pharr method [16]. The Vickers microhardness (microindentation) of the glasses was also estimated (measurement error ± 5%) using a micro-indentation hardness testing instrument (UHL VMHT, Walter UHLTM). For each sample, ten (10) micro-indentions were taken with a constant spacing of 10 μm under identical loading conditions (=500 g) under a 10 s dwell time [4]. The diagonal of different indents was carefully measured using an optical microscope attached to the instrument, and consequently the microhardness values were calculated using the standard Equation (1) for the Vickers geometry.

$$HV = \frac{1.854P}{d^2} \quad (1)$$

where *HV* is the Vickers hardness number (VHN) in Kg/mm^2. *P* is the normal load in g, *d* is the average diagonal length of the indentation in mm. Here, the *HV* value obtained/100.1 = Vickers hardness in GPa.

3. Results and discussion

In order to ensure the nucleation of chromium (Cr^{6+}) with respect to phase

transformation phenomena in Al_2O_3-SiO_2-MgO-B_2O_3-K_2O-F system, a non-isothermal differential scanning calorimetric (DSC) study was conducted, and the representative thermograms are shown in **Figure 1** [4]. The DSC pattern of ASG-0Cr glass exhibited in **Figure 1a** is very different compared to the chromium-doped one, i.e., the ASG-2Cr system (exhibited in **Figure 1c**). As seen from **Figure 1a**, the characteristic endothermic hump corresponding to the glass transition region is initiated at 580–590 °C and ended towards the minimum at 625–627 ℃. From the onset of that endothermic hump, the glass transition temperature (Tg) is estimated at 610 ± 2 ℃ for ASG-0Cr glass. In the case of the chromium-doped system, the appearance of the glass transition hump (DSC) presented in **Figure 1c** is very different compared to ASG-0Cr. The hump for ASG-2Cr in **Figure 1c** is insignificant to define those as amorphous material; however, the minor endothermic hump that appeared is the indication of residual Al_2O_3-SiO_2-MgO-B_2O_3-K_2O-F glassy phase [1,2]. As mentioned in the experimental section, after melting, the as-quenched glass was annealing heat-treated. After annealing, ASG-2Cr found crystallized. In the present system, the ASG-0Cr glass is not crystallized upon annealing temperature. It is a well-established fact that nucleation is the process by which atoms or molecules come together to form a new phase or structure, and such a process is the initial stage in the formation of a crystal and involves the formation of a small cluster of atoms or molecules, i.e., a nucleus. Hence, it can be elucidated that ASG-0Cr is practically glass, but ASG-2Cr is not glass; it can be a glass-ceramic composite [8,9], and the pattern of exothermic peak broadening in **Figure 1c** is due to a minor residual glass phase. In a similar study on boro-silicate systems, Aktas et al. [8] argued that 0–1 wt% Cr_2O_3 containing silicate glass is completely amorphous, but Cr_2O_3 contents >1 wt% make those glass crystalline. For ASG-0Cr glass, the exothermic maximum (peak) is estimated at 768 ± 2 ℃, which is corresponding to crystallization temperature [9]. Lin et al. [3] similarly studied DSC on Cr-doped alumino-silicate glass and argued that the incorporation of Cr-ion, as a modifier, can break the glass network and finally result in the decreased glass phase (i.e., Si-O-Si) stability. Thus, from DSC it is pointed out that the ASG-0Cr is glass but the ASG-2Cr contains crystallinity [4].

The nucleation phenomena of chromium (Cr^{6+}) doped Al_2O_3-SiO_2-MgO-B_2O_3-K_2O-F glass predicted from the DSC study were further confirmed from the X-ray diffraction (XRD) study [17]. XRD analysis revealed the formation of spinel phases at nucleation temperatures. As is evident from **Figure 1b** (i.e., ASG-0Cr glass), the broad hump that appeared at (2θ) 20°–35° signifies the amorphous nature. In view of the DSC experiment (**Figure 1**), it is pointed out that the catalyzed nucleation for initiating the crystallization process occurred in chromium-containing glass. Thus, crystalline nature is demonstrated by ASG-2Cr, as depicted in **Figure 1d**. As evident from **Figure 1d**, the crystalline peaks that appeared at (2θ) 18°, 30°, 36°, 37°, 44°, 58° and 63° are attributed to the crystalline planes (111), (220), (311), (222), (400), (511) and (531) of the spinel phase, $MgCr_2O_4$; JCPDS-PDF file number = 82–1529, FCC lattice [5]. The characteristic peaks appeared at (2θ) 18°, 30°, 36°, and 53° and are attributed to the formation of crystalline planes (101), (200), (202), and (312) of K_3CrF_6; JCPDS-PDF file number = 27–1354, tetragonal BCC lattice. ASG-2Cr is hence a glass-ceramic or glass-ceramic composite of multi-crystalline nature [4]. During the annealing at 600(±10) °C, MgF_2 crystals are precipitated as primary

crystalline phase, and the characteristic peaks (2θ) 36°, 40°, 44°, 53°, and 63° are ascribed to the (101), (111), (210), (211), and (310) crystalline planes of MgF_2, JCPDS-PDF file number = 72–2231. Another Al- and Si-enriched crystalline phase is also developed in these glasses during annealing at 600(±10) °C. The crystalline peaks formed at (2θ) 23°, 26°, 30°, 33°, 37°, 40° and 58° correspond to the crystalline planes (200), (120), (001), (220), (130), (121) and (041) of mullite ($3Al_2O_3{\cdot}2SiO_2$), JCPDS-PDF file number = 82–0037 [4]. For the ASG-2Cr system, the crystalline peak that appeared at (2θ) 36° is associated with the highest intensity, and that peak is ascribed to the development of the spinel phase ($MgCr_2O_4$) [4,16]. Thus, from XRD, it can be clarified that through the annealing heat treatment in such Al_2O_3-SiO_2-MgO-B_2O_3-K_2O-F system, the spinel phase, i.e., $MgCr_2O_4$ can be predominately obtained when using Cr^{6+} as a nucleation agent [6–9].

The Cr-controlled nucleation at annealing temperature was caused by chromium ions in the ASG-2Cr system, and thus the microstructures (FESEM) developed in such chromium-doped glass ceramic were studied. **Figure 2** presents the results of experimental investigation on microstructure (size and morphology of crystalline phases) [4]. As observed in **Figure 2a**, the randomly distributed crystallite particles throughout the matrix gathered to develop a colony-like arrangement. Under higher magnification, i.e., from **Figure 2b**, it is seen that rock-like 200-500 nm-sized crystalline particles are dispersed throughout the ASG system and further lead to a compact microstructure. From the EDX pattern (inset of **Figure 2b**), the elements present in the ASG-2Cr matrix are made out as K, O, Cr, Mg, Al, and Si, and it confirms the development of the predominant spinel phase ($MgCr_2O_4$), as already pointed out from XRD. Such fine-grained compact microstructure developed in the ASG-2Cr system significantly controls the mechanical parameters (microhardness, Young's mudulus, etc.) as analyzed from nanoindentation and microindentation studies [17,18].

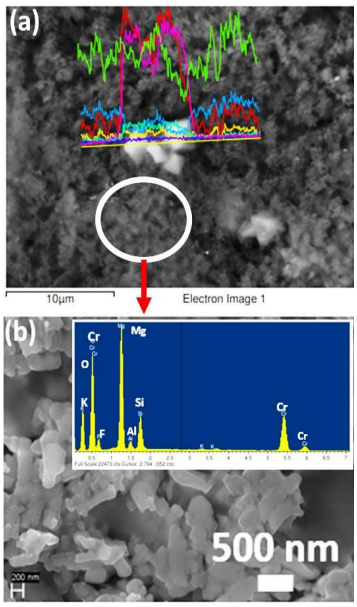

Figure 2. FESEM photomicrograph of Al_2O_3-SiO_2-MgO-B_2O_3-K_2O-F glass-ceramic (ASG-2Cr) in **(a)** 10 µm; **(b)** 500 nm scale (inset of **Figure 2b** presents the EDX pattern of ASG-2Cr system) [4].

The load-displacement curves and loading-unloading P-h curves from the nano-indentation tests on the studied glasses are presented in **Figures 3** and **4**, respectively. As pointed out from XRD and FESEM observations, the base Al_2O_3-SiO_2-MgO-B_2O_3-K_2O-F glass (Cr-0) is an amorphous system, which, on addition of chromium, was converted into the glass-ceramic, and such a similar observation is further evidenced from the load-displacement study exhibited in **Figure 3**.

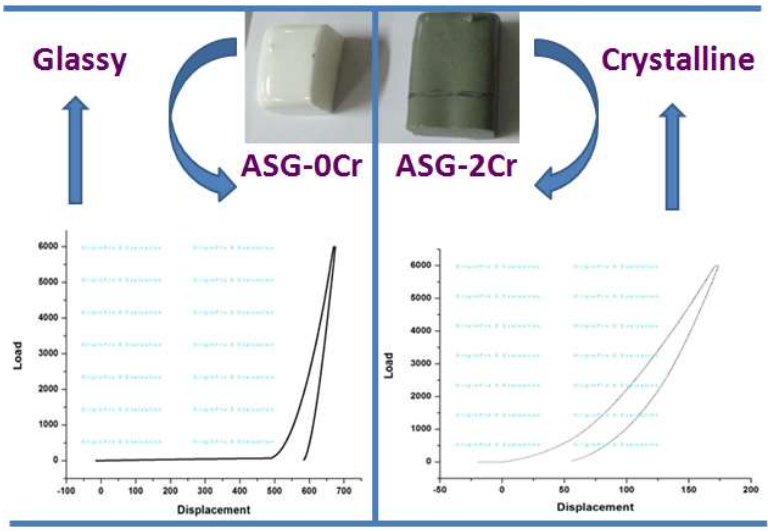

Figure 3. Load-displacement curves exhibiting ASG-0Cr as glass and CSG-2Cr as glass-ceramic.

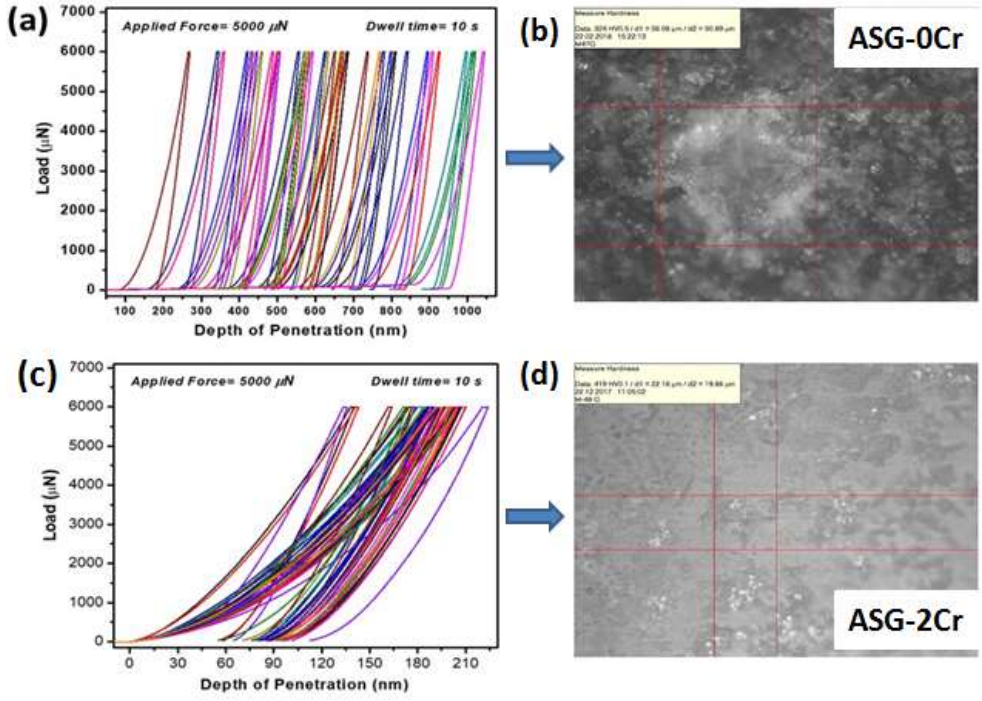

Figure 4. P-h curves from nano-indentation tests using Berkovich indenter tip from Al_2O_3-SiO_2-MgO-B_2O_3-K_2O-F glasses i.e., **(a)** ASG-0Cr; **(c)** ASG-2Cr. Photograph of Vickers microhardness indentation impression on; **(b)** ASG-0Cr; **(d)** ASG-2Cr glasses showing the increasing crystallinity with chromium content [4].

Figure 4a thus represents loading-unloading P-h curve characteristics for ASG-0Cr glass with a much higher depth of penetration for the constant load of 5 mN [4]. The low depth of penetration for ASG-2Cr glass-ceramics (**Figure 4c),** on the other hand, suggests higher strength due to correspondingly higher crystallinity and compactness of the microstructures [4]. The load-displacement curve also demonstrates the trend of increasing elastic modulus. The contact depth is the depth of indenter in contact with the ASG glass samples under used load *P* (constant load of 5 mN). When under the same load (*P*), a higher contact depth occurs, which means the sample is not so hard (comparatively), i.e., lower microhardness is observed [16,18]. For the ASG-0Cr system (glass), the depth of penetration reached to ~950 nm, whereas for ASG-2Cr glass-ceramics, it is ~200–250 nm. Interestingly, Young's modulus and microhardness both found to increase when Cr-ion was added to the base ASG glass (**Table 1),** and that is ascribed to the change in morphology of the crystal phases.

Table 1. Depth of penetration (*h*), Young's modulus and microhardness measured from the nano-indentation tests on Al_2O_3-SiO_2-MgO-B_2O_3-K_2O-F glasses with and without $K_2Cr_2O_7$ [4].

Sample	Contact depth (nm)	Young's modulus (GPa)	Microhardness (GPa)
ASG-0Cr	619 ± 195	25 ± 10	0.6 ± 0.5
ASGr-2Cr	139 ± 16	94 ± 21	8.4 ± 2.3

Microhardness Microhardness of glass/glass-ceramic materials is largely dependent on strength, crystallinity, as well as residual glass phase in the microstructure [17]. Vicker's microhardness indentation impression for the studied glasses is presented in **Figures 4b,d**. For ASG-0Cr glass, the microhardness is estimated at 3.63 (±0.18) GPa, and for chromium-containing systems, it is higher due to the crystalline nature [18]. The ASG-2Cr matrix (**Figure 2**) is composed of 200–500 nm-sized crystals dispersed randomly, and such arrangements are the reason for the microhardness value of 3.94 (±0.20) GPa [12,16].

Thus, the addition of Cr-ion caused self-nucleation and, moreover, a significant change in the microstructure and hence the mechanical properties, i.e., contact depth, modulus, and hardness value, of the ASG-2Cr system [18–20]. The residual glass phase in ASG-2Cr is directly related to the mechanical properties of such Al_2O_3-SiO_2-MgO-B_2O_3-K_2O-F glass ceramics [17,20]. This fact led to the suitability of ASG-2Cr glasses as a machinable glass-ceramic (MACOR) due to their specific microstructure-driven mechanical properties, including a microhardness of 3.94 ± 0.20 GPa [15–18].

4. Conclusions

In presence of chromium ion (Cr^{6+}), self-nucleation of Al_2O_3-SiO_2-MgO-B_2O_3-K_2O-F glass occurred at annealing heating 600 ± 10 °C only. From the XRD pattern, it is confirmed that the base glass is amorphous, whereas chromium-doped glass is crystalline with predominant phases of spinel ($MgCr_2O_4$). Dense and compact microstructure containing 200–500 nm crystallites is obtained in chromium-doped Al_2O_3-SiO_2-MgO-B_2O_3-K_2O-F glass ceramic. From nano-indentation, the hardness

and Young's modulus for base glass were estimated 0.6(±0.5) and 25(±10) GPa, respectively, which increased in the case of chromium-doped glass ceramics. Vicker's microhardness for the base glass was 3.63(±0.18) GPa which was also increased to 3.94(±0.20) GPa for chromium-containing glass ceramic. In brief, the hexavalent chromium ion (Cr^{6+}) doping in alumino-silicate glass Al_2O_3-SiO_2-MgO-B_2O_3-K_2O-F imposed nucleation at annealing temperature and was thereby effective for improving the machinability.

Author contributions: Conceptualization, MG; methodology, MG; data curation, MG and AAR; writing—original draft preparation, MG and AAR; writing—review and editing, SR. All authors have read and agreed to the published version of the manuscript.

Funding: The author is thankful to B. Karmakar, Former Head, GSTS, CSIR-Central Glass and Ceramic Research Institute, Kolkata for his guidance (PhD thesis) to carry out this work. MG thankfully acknowledges DST-SERB for financial support under the National Post Doctoral Fellowship (N-PDF) scheme (Ref No: PDF/2016/003799) at Indian Institute of Technology (IIT), Kharagpur. AAR is thankful for the partial support form University of Tetova.

Conflict of interest: The authors declare no conflict of interest.

References

1. Zarabi Golkhatmi S, Asghar MI, Lund PD. A review on solid oxide fuel cell durability: Latest progress, mechanisms, and study tools. Renewable and Sustainable Energy Reviews. 2022; 161: 112339. doi: 10.1016/j.rser.2022.112339
2. Beall GH. Milestones in Glass-Ceramics: A Personal Perspective. International Journal of Applied Glass Science. 2014; 5(2): 93-103. doi: 10.1111/ijag.12063
3. Lin C, Liu J, Han L, et al. Study on the structure, thermal and optical properties in Cr_2O_3-incorporated MgO-Al_2O_3-SiO_2-B_2O_3 glass. Journal of Non-Crystalline Solids. 2018; 500: 235-242. doi: 10.1016/j.jnoncrysol.2018.08.004
4. Garai M, Karmakar B, Roy S. Cr^{6+} Controlled Nucleation in SiO_2-MgO-Al_2O_3-K_2O-B_2O_3-F Glass Sealant (SOFC). Frontiers in Materials. 2020; 7: 57. doi: 10.3389/fmats.2020.00057
5. Pingale SS, Patil SF, Vinod MP, et al. Mechanism of humidity sensing of Ti-doped $MgCr_2O_4$ ceramics. Materials Chemistry and Physics. 1996; 46(1): 72-76.
6. Bremm S, Dölling S, Becker W, et al. A methodological contribution to failure prediction of glass ceramics sealings in high-temperature solid oxide fuel cell stacks. Journal of Power Sources. 2021; 507: 230301. doi: 10.1016/j.jpowsour.2021.230301
7. Sun, T, Chi Z, Feng Z, et al. Mixed CaO/MgO effect on microstructure, mechanical properties and crystallization behaviour of Li_2O-Al_2O_3-SiO_2-ZrO_2-P_2O_5 glass. Journal of Non-Crystalline Solids. 2023; 616: 122457. doi: doi.org/10.1016/j.jnoncrysol.2023.122457
8. Aktas B, Yalcin S, Dogru K, et al. Structural and radiation shielding properties of chromium oxide doped borosilicate glass. Radiation Physics and Chemistry. 2019; 156: 144-149. doi: 10.1016/j.radphyschem.2018.11.012
9. Timurkutluk C, Toruntay F, Onbilgin S, et al. Development of ceramic fiber reinforced glass ceramic sealants for microtubular solid oxide fuel cells. Ceramics International. 2022; 48(11): 15703-15710. doi: 10.1016/j.ceramint.2022.02.105
10. Garai M, Reka AA, Karmakar B, et al. Microstructure–mechanical properties of Ag0/Au0 doped K–Mg–Al–Si–O–F glass-ceramics. RSC Advances. 2021; 11(19): 11415-11424. doi: 10.1039/d0ra10519h
11. Das, S, Madheshiya A, Das S, et al. Mechanical, surface morphological and multi-objective optimization of tribological properties of V_2O_5 doped lead calcium titanate borosilicate glass ceramics. Ceramics International. 46(11): 19170-19180. doi: 10.1016/j.ceramint.2020.04.252
12. Karamanov A, Pisciella P, Pelino M. The effect of Cr_2O_3 as a nucleating agent in iron-rich glass-ceramics. Journal of European Ceramic Society. 1999; 19: 2641-2645. doi: 10.1016/S0955-2219(99)00047-3

13. Hubert M, Faber AJ, Akmaz F, et al. Stabilization of divalent chromium Cr(II) in soda-lime-silicate glasses. Journal of Non-Crystalline Solids. 2014; 403: 23-29. doi: 10.1016/j.jnoncrysol.2014.06.015
14. Singh K, Walia T. Review on silicate and borosilicate-based glass sealants and their interaction with components of solid oxide fuel cell. International Journal of Energy Research. 2021; 45(151): 20559-20582. doi: https://doi.org/10.1002/er.7161
15. Rezvani M, Eftekhari-Yekta B, Solati-Hashjin M, et al. Effect of Cr_2O_3, Fe_2O_3 and TiO_2 nucleants on the crystallization behaviour of SiO_2-Al_2O_3-CaO-MgO(R_2O) glass-ceramics. Ceramics International. 2005; 31(1): 75-80. doi: 10.1016/j.ceramint.2004.03.037
16. Oliver WC, Pharr GM. An improved technique for determining hardness and elastic modulus using load and displacement sensing indentation experiments. Journal of Materials Research. 1992; 7(6): 1564-1583. doi: 10.1557/jmr.1992.1564
17. Garai M, Murthy TSRCH, Karmakar B. Microstructural characterization and wear properties of silver and gold nanoparticle doped K-Mg-Al-Si-O-F glass-ceramics. Ceramics International. 2018; 44(18): 22308-22317. doi: 10.1016/j.ceramint.2018.08.356
18. Jahanshahi M, Mofidian R, Hosseini SS, et al. Investigation of mechanical properties of granular γ-alumina using experimental nano indentation and nano scratch tests. SN Applied Sciences. 2023; 5(6). doi: 10.1007/s42452-023-05388-7
19. Garai M, Singh CK, Rout SK. Crystallization and microstructure in K_2O substituted SiO_2-MgO-Al_2O_3-Li_2O-$AlPO_4$ glass-ceramics. Solid State Communications. 2022; 350: 114758. doi: 10.1016/j.ssc.2022.114758
20. Serbena FC, Mathias I, Foerster CE, et al. Crystallization toughening of a model glass-ceramic. Acta Materialia. 2015; 86: 216-228. doi: 10.1016/j.actamat.2014.12.007